Mesoscale Mapping Capabilities of Multiple-Satellite Altimeter Missions

P. Y. LE TRAON AND G. DIBARBOURE

CLS Space Oceanography Division, Ramonville St. Agne, France

(Manuscript received 20 April 1998, in final form 11 November 1998)

ABSTRACT

The purpose of this paper is to quantify the contribution of merging multiple-satellite altimeter missions to the mesoscale mapping of sea level anomaly (*H*), and zonal (*U*) and meridional (*V*) geostrophic velocities. A space/time suboptimal interpolation method is used to estimate the mean and standard deviation of the *H, U,* and *V* mapping errors (as a percentage of signal variance) for different orbit configurations. Only existing or planned orbits [TOPEX/Poseidon (T/P), *Jason-1, ERS-1/2*–ENVISAT, Geosat–GFO] are analyzed. *Jason-1* and T/P orbits are assumed to be interleaved. A large number of simulations are performed, including studies of sensitivity to a priori space scales and timescales, noise, and latitude. In all simulations, the Geosat orbit provides the best sea level and velocity mapping for the single-satellite case. In most simulations, the *Jason-1*–T/P orbit provides the best two-satellite mapping. However, the gain from an optimized two-satellite configuration (*Jason-1* + T/P) compared to a nonoptimized configuration (T/P + ERS or T/P + Geosat) is small. There is a large improvement when going from one satellite to two satellites. Compared to T/P, the combination of T/P and ERS, for example, reduces the *H* mean mapping error by a factor of 4 and the standard deviation by a factor of 5. Compared to ERS or even Geosat, the reduction is smaller but still by a factor of more than 2. The *H* mapping improvement is not as significant when going from two to three or three to four satellites. Compared to the Geosat, ERS, and T/P mean mapping errors, the *Jason-1* + T/P mean mapping error is, respectively, reduced by 5%, 9%, and 17% of the signal variance. The reduction in mean mapping error by going from two to three and from three to four satellites is, however, only 1.5% and 0.7% of the signal variance, respectively. These results differ from Greenslade et al. mainly because of the definition of resolution adopted in their study. The velocity field mapping is also more demanding in terms of sampling. The *U* and *V* mean mapping errors are two to four times larger than the *H* mapping error. Only a combination of three satellites can actually provide a velocity field mean mapping error below 10% of the signal variance. The mapping of *V* is also less accurate than the mapping of *U* but by only 10%–20%, even at low latitudes. These results are confirmed using model data from the Parallel Ocean Climate Model (POCM). POCM *H, U,* and *V* are thus very well reconstructed from along-track altimeter data when at least two satellites are used. The study also shows that the *Jason-1*–T/P orbit tandem scenario has to be optimized taking into account the other satellites (GFO and ENVISAT). It also confirms the usually agreed upon main requirement for future altimeter missions: at least two (and preferably three) missions (with one very precise long-term altimeter system to provide a reference for the other missions) are needed.

1. Introduction

Over the last five years, several altimeter satellites (TOPEX/Poseidon, *ERS-1*, and *ERS-2*) have been flying simultaneously. This will recur in the future with the Geosat follow-on (GFO), ENVISAT, and *Jason-1* missions. While TOPEX/Poseidon (T/P), with its unprecedented accuracy, has provided a new picture of the ocean, it cannot observe the full spectrum of the sea level and ocean circulation variations. Only a combination of several altimeter missions will resolve the main space and timescales of the ocean circulation, in particular the mesoscale ocean circulation. Several studies have shown that a two-altimeter combination is needed for a better representation of the eddy field (e.g., Chassignet et al. 1992; Blayo et al. 1997). More theoretical analyses of the sampling or resolution capabilities of single- or multiple-altimeter missions have also been carried out (e.g., Wunsch 1989; Greenslade et al. 1997). The results are not always consistent, however, and are often sensitive to the method used for assessing the contribution of altimeter data. This is particularly true when using data assimilation techniques, whose results are often representative of the model/assimilation skill rather than the true capability of the observing system. Although the latter techniques should be used ultimately to determine the impact of altimeter data, it is still useful and necessary to quantify the contribution of the data themselves.

Recently Greenslade et al. (1997, hereafter GCS97)

Corresponding author address: Dr. P. Y. Le Traon, CLS Space Oceanography Division, 8-10 rue Hermes, Parc Technologique du Canal, 31526 Ramonville St. Agne, France.
E-mail: letraon@cls.cnes.fr

analyzed the resolution capability of sea surface height (SSH) fields constructed from single- and multiple-satellite altimeter missions. The main criterion was that the expected squared errors over the space–time grid should be homogeneous to within 10% (maximum–minimum of errors below 10% of the mean squared error). It was shown that the mapping resolution capabilities of non-optimized combined datasets (such as T/P and *ERS-1/2*) were not significantly better than those of fields constructed from T/P alone. The criterion chosen for defining the resolution capability partly explains this unexpected conclusion. It requires a very homogeneous mapping error. As a result, only large-scale signals can be ''resolved'' and GCS97 conclude that mesoscale variability cannot be mapped with acceptable accuracy with any of the existing or future multiple-altimeter missions. Choice of criteria for the assessment of the mapping capability is, however, a subjective decision, and we will argue that mesoscale variability can be rather well mapped from multiple-altimeter missions.

The purpose of this paper is thus to quantify the contribution of merging one, two, three, and four satellite altimeter missions to the mesoscale mapping of sea level anomaly (H), and zonal (U) and meridional (V) geostrophic velocities. It also aims to provide useful results for the choice of the T/P–*Jason-1* tandem mission scenario. Optimal interpolation will be used to determine the mapping error of the different existing orbit configurations (T/P–*Jason-1, ERS-1/2*–ENVISAT, Geosat–GFO). We will not take into account the differences in error budgets and will only analyze the sampling characteristics of the orbits (not the missions). The differences in error budgets could be, however, partly reduced prior to or during mapping by using, for example, the more precise mission (T/P and later on *Jason-1*) as a reference for the other missions (e.g., Le Traon and Ogor 1998; Le Traon et al. 1998). Results obtained should thus remain valid for missions with different error budgets. This also means that the unique contribution of T/P and later on *Jason-1* will be to provide a reference for the other missions (constraint on the large-scale signal). The different altimeter missions will then provide complementary space/time sampling of the ocean, which is the very subject of this paper.

This paper is organized as follows. Methods are presented in section 2. Section 3 shows the results and discusses their sensitivity to the a priori choice of space and time correlation functions, a priori noise, and latitude. Model simulations are used in section 4 to verify the results. Main conclusions are given in section 5.

2. Methods

Optimal interpolation is an effective way of testing a sampling strategy (Bretherton et al. 1976). The mapping error depends on the space/time location of the observation points and on the a priori space and time covariance function of the signal and noise. The mapping error will be realistic only when the a priori covariance functions are well chosen. These functions are rather well known, thanks to statistical analyses of altimeter data (e.g., Le Traon 1991; Stammer 1997). As they depend on geographical position (e.g., latitude), our calculation will not be limited to a single space scale and timescale but will use a range of possible values.

a. Optimal interpolation method

A space/time suboptimal objective analysis of along-track altimeter sea level anomaly (H) data as described in Le Traon and Hernandez (1992) or Le Traon et al. (1998) will be used. This method is similar to a conventional optimal interpolation method (Bretherton et al. 1976) except in the suboptimality. For our application, along-track altimeter data will be selected in a sphere of influence whose radius is equal to the space scale (L) and timescale (T) of the ocean signal (see the exact definitions of L and T below). Along-track data are also undersampled (one point in three) to reduce the computational load. Note that results will be similar to a full along-track sampling with a measurement noise level variance multiplied by three. We assume here a noncorrelated noise of 10% of signal variance for the different satellites (tests will be done with a reduced noise level of 2%).

b. Zonal and meridional velocity

We will also analyze the mapping error on the zonal (U) and meridional (V) geostrophic velocities. This can easily be done with the same mapping procedure by modifying the correlation function between the field to be mapped (i.e., U or V in place of H) and the observations (H) (see Le Traon and Hernandez 1992). If we assume geostrophy, only the H covariance function $C(r, t)$ needs to be known, as the correlation between U, V, and H can be directly derived from C (e.g., Le Traon and Hernandez 1992). As the covariance between U or V and H is related to the first derivative of C, the estimation of the velocity mapping error is more sensitive, however, to the a priori choice of the covariance function.

c. Correlation function

The following space–time correlation function $C(r, t)$ of the sea level anomaly field already used by Le Traon and Hernandez (1992) and Le Traon et al. (1998) will be used:

$$C(r, t) = [1 + ar + (1/6)(ar)^2 - (1/6)(ar)^3] \exp(-ar) \times \exp(-t^2/T^2),$$

where r is distance, t time, $L = 3.34/a$ the space correlation radius (first zero crossing of C), and T the temporal correlation radius. The nominal values of L and

T will be set to 150 km and 15 days, respectively, scales typical of mesoscale ocean circulation. Tests will be done with *L* ranging from 75 to 225 km and *T* ranging from 10 to 20 days.

d. Methods

Error maps will be calculated on a 10° × 10° area (between 40°–50°N) every 5 days over 35 days (eight maps) for different satellite orbit configurations. The grid spacing is 0.2°. The space and time mean error (expressed as a percentage of signal variance) and the standard deviation of the error will then be calculated for *H*, *U*, and *V*. As an illustration, Fig. 1 shows the error maps on *H* obtained for the Geosat–GFO orbit.

Tests will also be done on a different latitude band between 10° and 20°N to analyze the difference in sampling according to latitude (influence of intertrack distance and track inclination).

Figure 2 shows the tracks of the different satellites (*ERS-1/2* or ENVISAT, T/P, *Jason-1*, Geosat or GFO). The *Jason-1* and T/P orbits are assumed to be interleaved. This is one possible scenario for the tandem phase of T/P and *Jason-1* (*Jason-1* will fly along the T/P track after the tandem phase). It can be considered, however, as an optimal sampling design for a two-satellite configuration. Another scenario would be to have T/P and *Jason-1* covering the same ground track, but this solution would be less suitable for sampling issues (except for some specific ocean signals) and will not be analyzed here.

3. Results

a. Sea level anomaly mapping

Figure 3 gives the sea level anomaly mapping error and its standard deviation for the nominal values of *L* and *T* (150 km and 15 days) and for all tested orbit configurations. Geosat gives the best results for the single-satellite case and provides a good mapping. The mean error is only 10%, which is the a priori along-track error, and the standard deviation of the error is 5%. ERS errors are larger. TOPEX/Poseidon (or *Jason-1*) has the largest error. This was expected as the T/P orbit was optimized for the large-scale ocean signal observation and not for mesoscale variability mapping. Note that the error structures in these three cases are very different. Because the repeat period of T/P is short compared to the a priori timescale *T*, T/P error is very homogeneous over time but has large spatial variability. ERS errors, and to a lesser extent Geosat, are more complex, however, exhibiting both spatial and temporal variability (see Fig. 1).

The *Jason-1* + T/P combination provides the best two-satellite configuration, but there is not much difference relative to the combinations of T/P + Geosat or T/P + ERS. Geosat, T/P, *Jason-1*, or ERS provide complementary sampling, which explains why combining two of these satellites enhances the mapping. Compared with T/P, the combination of T/P and ERS has, for example, a mean mapping error reduced by a factor of 4 and a standard deviation reduced by a factor of 5. Compared to ERS, the reduction is smaller but still a factor of more than 2.

The two three-satellite configurations (T/P + ERS + Geosat and T/P + ERS + *Jason-1*) have almost the same mapping errors. Compared to the two-satellite configurations, the mapping error is reduced by about 30%. The four-satellite configuration reduces error slightly more again. The main result, however, is that there is a large improvement when going from one to two satellites. Three or even four satellites are still useful but the increase in mapping accuracy from two to three or four is less significant. Compared to the Geosat, ERS, and T/P mean mapping errors, the *Jason-1* + T/P mean mapping error is, respectively, reduced by 5%, 9%, and 17% of the signal variance. The reduction in mean mapping error by going from two to three and from three to four satellites is, however, only 1.5% and 0.7% of the signal variance, respectively.

b. Comparison with Greenslade et al. (1997) results

Contrary to GCS97 results, there is thus a very clear improvement due to the merging of T/P and ERS and more generally due to the merging of multiple-altimeter missions. Note that the ratio *R* of the standard deviation of error over the mean mapping error is typically around 0.5 for most of the configurations we analyzed. GCS97 require that the ratio maximum–minimum of errors over the mean mapping error to be 0.1, which means that (for Gaussian distribution) they require an *R* of 0.03. This may be a sensible choice, but, as a result, only large-scale signals can be ''resolved.'' To get such a ratio, we need, as in GCS97, to smooth the data, that is, to use correlation functions with much larger space scales and timescales than the actual (mesoscale) signal. GCS97 thus find that the mesoscale signal cannot be resolved. One may argue about the resolution of the mesoscale signals (see discussion below). Still, it is useful to quantify the improvement of the mesoscale mapping when merging several altimeter datasets. This is not done in GCS97 but can be extrapolated from results shown at bottom left corners of their mean RESB and %RESB figures (i.e., at the highest analyzed spatial and temporal resolutions). There, the comparison of the different satellites configurations is more in agreement with our findings. Our conclusions are thus different from those of GCS97 mainly because the contribution of the merging for mesoscale and large-scale mapping is quite different.

According to GCS97 definition, none of our configurations (even those with four satellites) can resolve the ocean mesoscale variability. While the paper does not deal with the resolution capability (in that sense, it is

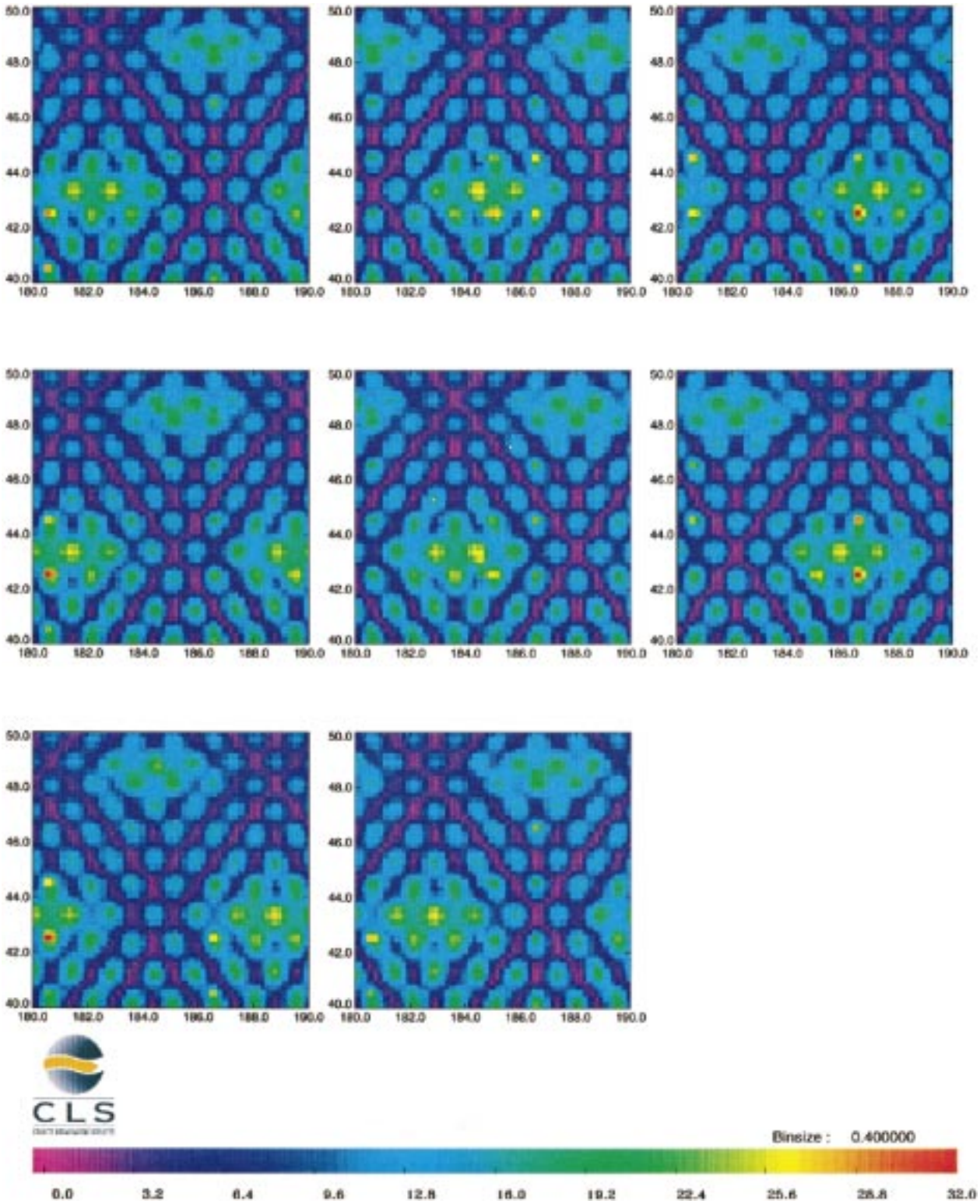

FIG. 1. Mapping error on sea level anomaly (H) for the Geosat orbit configuration. There is one map every five days. Units are percentages of signal variance.

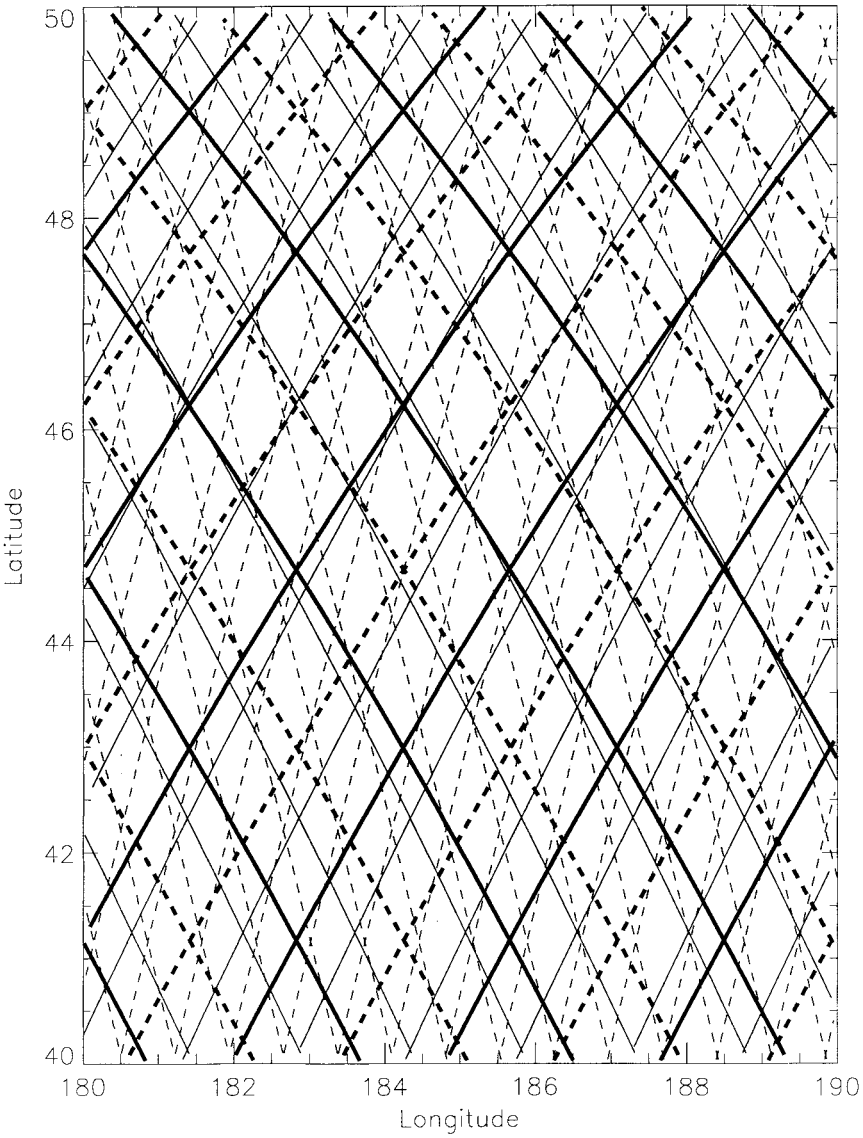

FIG. 2. The study area with the tracks of the different satellite orbits superimposed (T/P is the bold line, *Jason-1* is the dotted bold line, ERS–ENVISAT is the dotted line, and Gesoat–GFO is the thin line).

less ambitious than the GCS97 approach), we think, however, that mesoscale signals are rather well or well resolved by merging several altimeter datasets. All the two-satellite configurations we analyzed have mean mapping errors, for example, comparable to that obtained with dense hydrographic arrays (e.g., Hernandez et al. 1995). The mapping errors are always less than the a priori along-track error, and the maximum error is always below 20% of the signal variance. The three satellite configurations typically have a mean mapping error of 3% of the signal variance and a standard deviation of the error of 1.5% ($R = 0.5$). This means that for a signal of 10 cm rms, the mapping error will be between 1.2 and 2.1 cm (at one standard deviation). Such mapping errors will allow a very good tracking of most of the eddies since the mapping error will be always much smaller than the signal to be mapped. GCS97 requires a ratio R of 0.03, that is, assuming the same mean mapping error, a standard deviation of error of 0.09%. That is, for this particular example, an error between 1.71 and 1.73 cm (which is a very homogenous mapping error). They thus require to have almost everywhere the same mapping error. It is very clear that the mesoscale signal will be always better estimated along the tracks, but even if the mapping error is increased by a factor of 2 between the tracks, this may be acceptable if the error remains below a certain threshold (compared to the signal variance). As discussed by

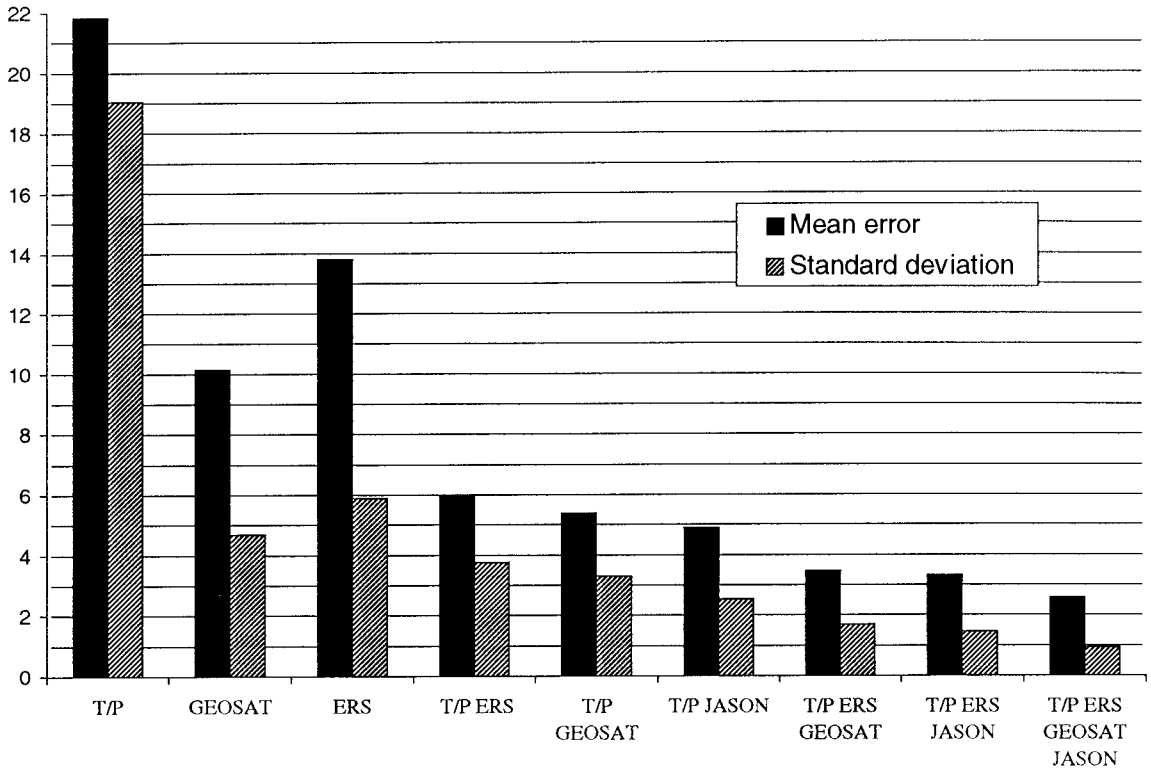

FIG. 3. Mean and standard deviation of sea level anomaly mapping error for single- and multiple-altimeter missions. Units are percentages of signal variance.

GCS97, the mapping error spatial and temporal inhomogeneity can be ignored if the overall mapping error is deemed to be acceptably small. GCS97 chose a criterion of 1% for the mean squared mapping error. We also believe that the spatial and temporal inhomogeneity criterion can be considerably relaxed (but not necessarily ignored) when mean mapping errors are below a certain threshold. A reasonable and less demanding—but also subjective—alternative to the GCS97 criterion could thus be to have mapping errors always below 10% of the signal variance, regardless of the inhomogeneity of the mapping error. Our results show that this criterion is met by all three satellite configurations.

c. Zonal and meridional velocity mapping

The structure of the mapping error on *U* or *V* and *H* is very different. This is exemplified in Fig. 4, which shows the mapping error on *H*, *U*, and *V* for the T/P configuration. First, the error on *U* and *V* is larger (more than 40% of the signal variance) than for *H* (20% of signal variance). As expected, estimating a derivative is more difficult than estimating the signal itself and is more demanding in terms of sampling (see the appendix). The standard deviation of the error is, however, smaller because the error is more evenly distributed in space. The along-track data are not sufficient to estimate the velocity field and data from neighboring tracks are needed. As a result, the error is more homogeneous but larger than for *H*. The minimal errors for *U* and *V* are actually found near crossover points, where sea level gradients are best estimated. The structure of *U* and *V* errors is also different. Near a crossover point, the zonal sea level gradients are best estimated in the north–south direction, which explains the elongated north–south structure of the *V* errors.

These main characteristics are found for all tested orbit configurations (Figs. 5 and 6). The structures of *U, V,* and *H* errors are very different; the *U* and *V* mean mapping errors are between two to four times larger than for *H*, and the *U* and *V* standard deviations are smaller than the *H* standard deviation. The ratio of standard deviation to mean mapping error is thus typically three or four times smaller for *U* and *V* compared to *H*. The ranking of the different configurations in terms of sampling is, however, similar. The only slight difference is that the T/P + Geosat combination has a slightly smaller mean error on *V* and *U* compared to the *Jason-1* + T/P configuration. The error on *V* is always larger than the error on *U* but by 10% only. Calculating the two components of the velocity field at crossover points yields a *V* noise variance larger than *U* noise variance by a factor of $(1/\tan\theta)^2$, where θ is the angle between the ground track and the north meridian (which depends on latitude) (e.g., Morrow et al. 1994). For our latitude band (see also the results for the latitude band between

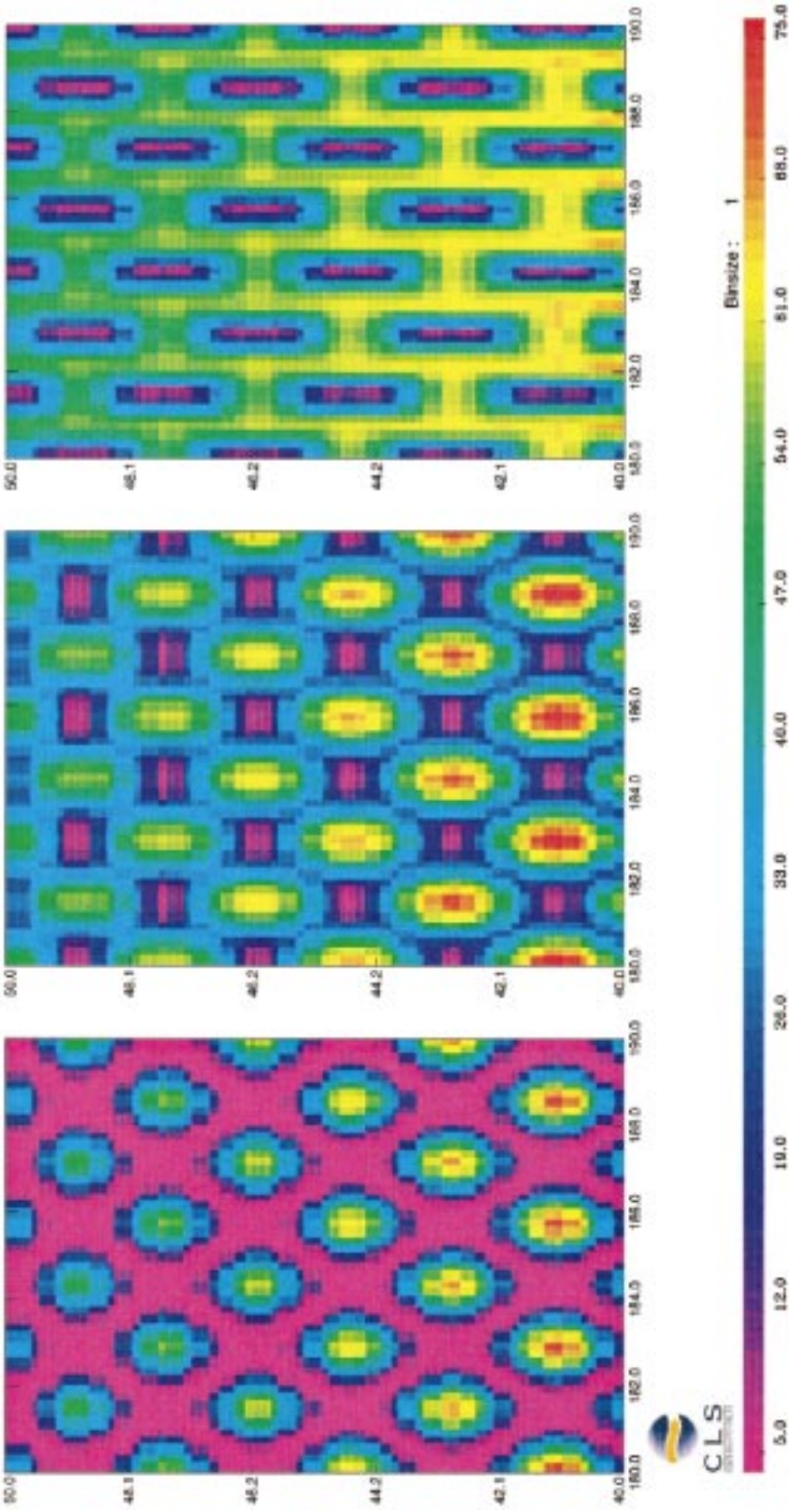

FIG. 4. Comparison of the mapping error on H, U, and V for the T/P orbit configuration. Units are percentages of signal (H, U, or V) variance.

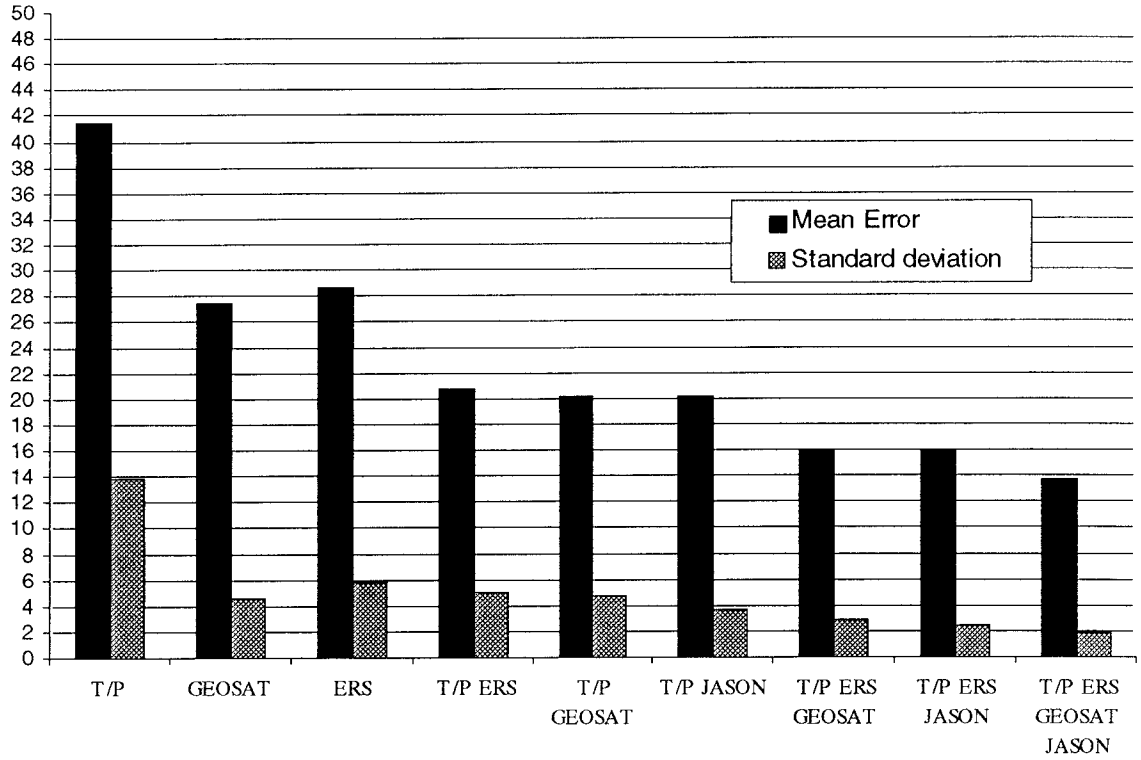

FIG. 5. Mean and standard deviation of zonal geostrophic velocity (U) mapping error for single- and multiple-altimeter missions. Units are percentages of signal variance.

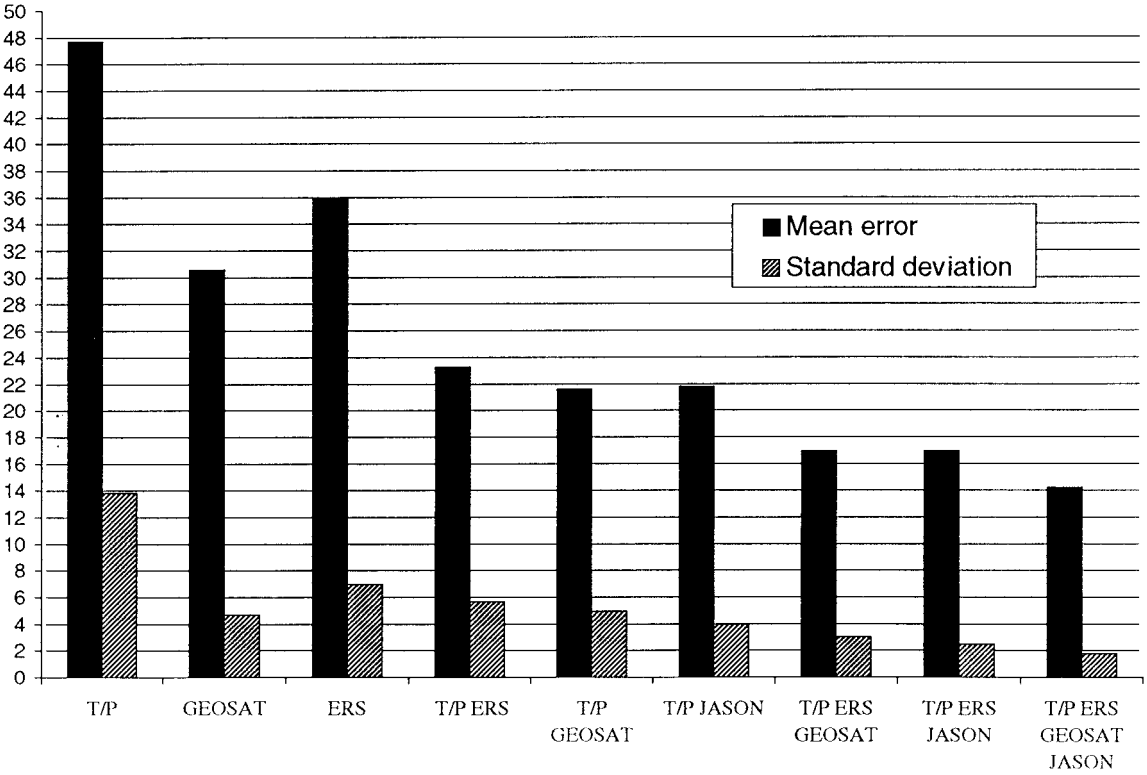

FIG. 6. Mean and standard deviation of zonal geostrophic velocity (V) mapping error for single- and multiple-altimeter missions. Units are percentages of signal variance

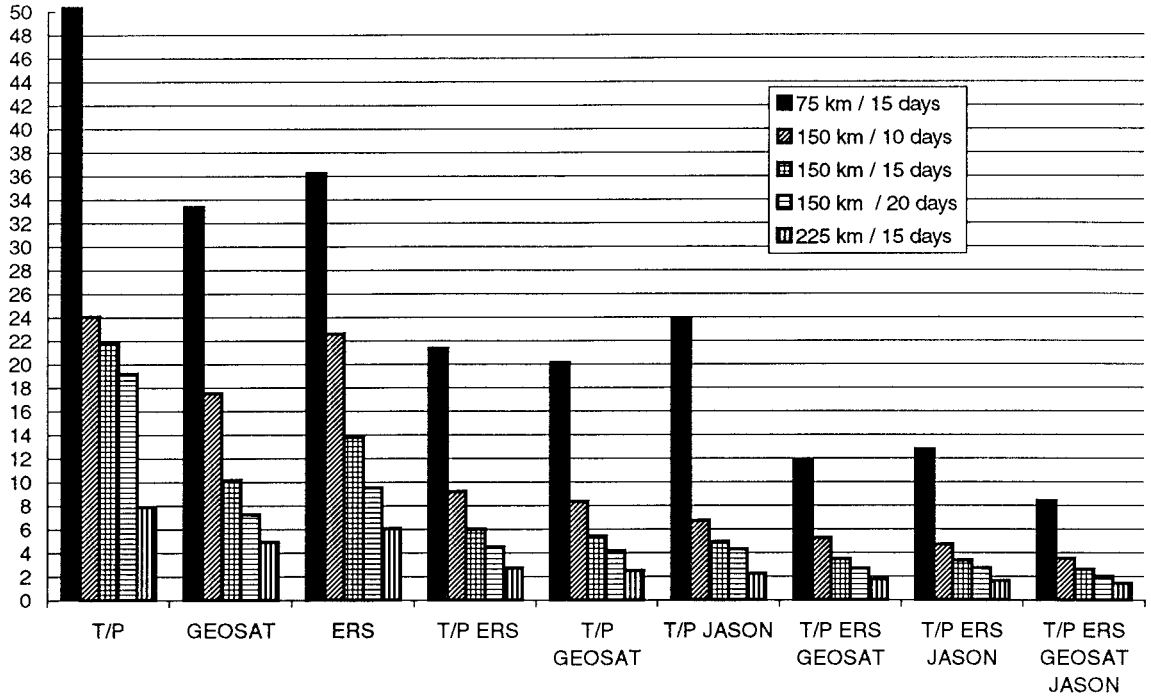

FIG. 7. Mean of sea level anomaly (H) mapping error for single- and multiple-altimeter missions for different a priori space scales and timescales. Units are percentages of signal variance.

10° and 20°), this yields a V noise variance almost three times larger than the error on U for the Geosat orbit configuration. The difference in mapping error between V and U is much smaller (between 10% and 20%) because (i) it represents both the noise and (mainly) the sampling error variances and (ii) the adjacent and crossing tracks suitably constrain estimates of the zonal sea level gradient and thus of the meridional velocity V at any grid point. This also shows that the criterion of a satellite orbit with a rather low inclination for a better estimation of the velocity field is not really relevant, in particular for a multisatellite configuration.

d. Sensitivity to correlation scales

Four other calculations with different space scales (L) and timescales (T) were performed to analyze the sensitivity of the results to different correlation scales. Two calculations use different timescales (10 and 20 days) and the same space scale as the nominal case (150 km). The other two use the same timescale as the nominal case (15 days) and two different space scales (75 and 225 km). These values cover the most likely ranges of mesoscale variability space and timescales (e.g., Le Traon 1991; Stammer 1997). Results for H mean mapping error are given in Fig. 7. The error varies considerably according to the correlation function. For example, it is reduced by up to a factor of 6 when going from $L = 75$ km, $T = 15$ days to $L = 225$ km, $T = 15$ days. The ranking of the different configurations is generally not modified, although for the case $L = 75$ km, $T = 15$ days, the T/P + Geosat or T/P + ERS configurations give better results than the *Jason-1* + T/P configuration. The different configurations do not have the same sensitivity, however, to the change in correlation function. For example, T/P is virtually insensitive to our timescale change, while ERS is more sensitive. These characteristics are also found in the two-satellite configurations.

e. Sensitivity to noise and latitude

Studies of sensitivity to the a priori noise and to the latitude were also performed. Figure 8 shows the ratio of mean mapping error with an a priori noise of 2% over mean mapping error with an a priori noise of 10%. As expected, the mapping error is reduced when using an a priori noise of 2%. The reduction factor is less than 2 (although noise is reduced by a factor of 5). This factor is larger when more satellites are sampling the sea surface and smaller for the velocity field. The differences between the one- and two- and two- and three-satellite results are thus increased. This is because when the signal is quite well sampled (e.g., with at least two satellites), the percentage of the mapping error due to the a priori noise is greater. This also explains why the mapping error is reduced less for the velocity field, which is more demanding in terms of sampling. The same explanation holds for the larger reduction in error for U compared to V. The *Jason-1* + T/P configuration

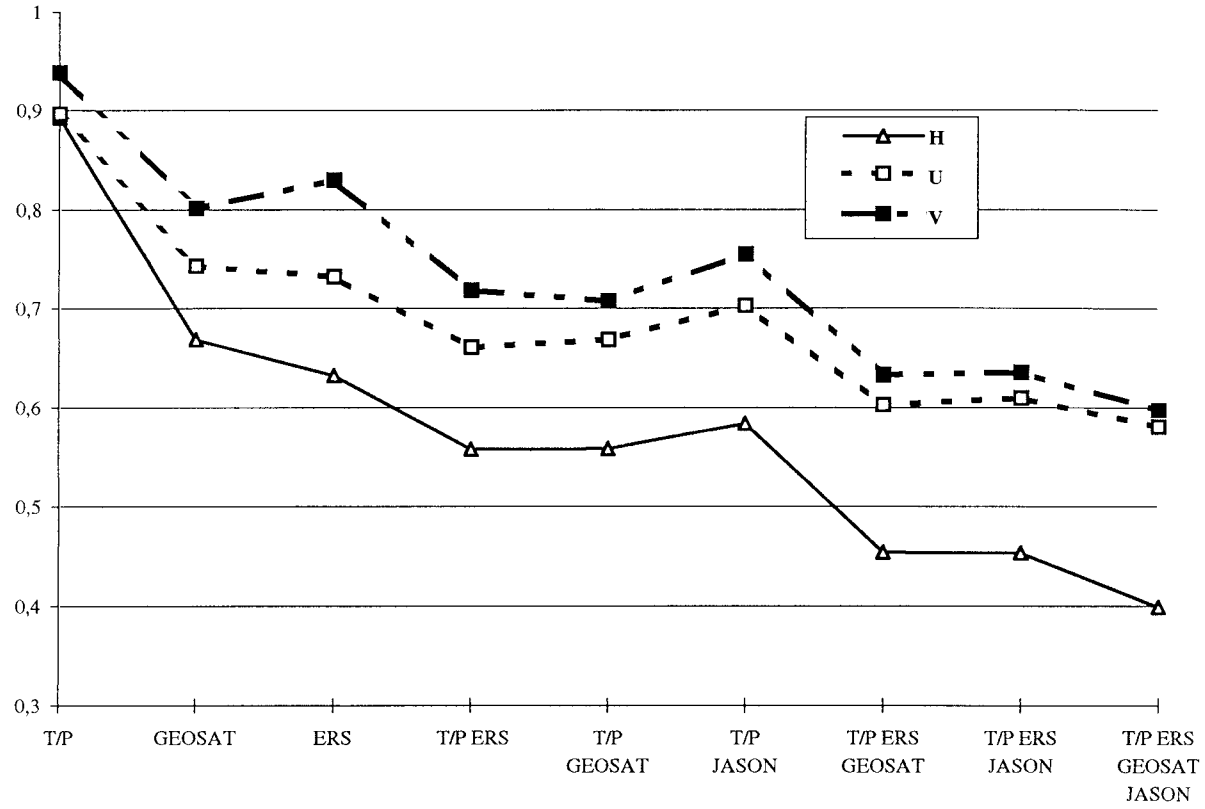

FIG. 8. Ratio of the *H* mean mapping error with an a priori noise of 2% over the *H* mean mapping error with an a priori noise of 10%.

is also slightly less sensitive than the T/P + ERS or T/P + Geosat orbit configuration. With an a priori noise of 2%, the T/P + Geosat orbit configuration provides a better mapping of the velocity field (*U* and *V*) than the *Jason-1* + T/P configuration. This actually was already noted with an a priori noise of 10%, but the effect is now greater.

Figure 9 shows the ratio of the *H* mean mapping error for the latitude band (10°–20°) over the *H* mean mapping error for the nominal (40°–50°) latitude band. The mean mapping error is larger in the 10°–20° band (for the same a priori space scales and timescales) as the tracks are farther apart (note, however, that in reality the a priori space scales are larger, which should reduce the effect). The error on the velocity field is also modified because of the change in the track inclination (the Coriolis parameter also is smaller, but this should not impact the relative mapping error; see the appendix). The error on *V* increases more than the error on *U* (except for ERS) because of the change in track inclination. The variation in latitude does not affect the different orbit configurations in the same way. The ERS orbit configuration, in particular, is less sensitive to the change in latitude than T/P and Geosat. This is clearly observed for the one- and two-satellite configurations. In fact, the T/P + ERS configuration is the best two-satellite configuration for this latitude band and for the nominal choice of *L* and *T* (which are not really realistic in this latitude band). This is because the other configurations clearly do not provide adequate spatial sampling. The *U* and *V* mapping errors are also proportionally less sensitive than the *H* mapping error to latitude, but we must remember that the errors on *U* and *V* are much larger than the error on *H*.

4. Verification of results using POCM model data

To further illustrate the capability of mesosale signal mapping from multiple-altimeter missions, a simulation using Parallel Ocean Climate Model (POCM) outputs is performed. As in GCS97, the model used is the run 11 of the primitive equation, multilayer model developed by the Parallel Ocean Program (POP) at Los Alamos National Laboratory (Dukowicz and Smith 1994). We chose an area dominated by mesoscale variability in the Gulf Stream extension between 36° and 41°N and 65° and 55°W. The model sea level outputs were first transformed into sea level anomaly data by removing a 3-yr mean. They were then subsampled to obtain simulated along-track altimeter datasets for T/P, *Jason-1*, ERS, and GFO. Those simulated datasets were then used to reconstruct the sea level anomaly gridded fields using the optimal interpolation method presented in section 2. The covariance functions are those used for our nom-

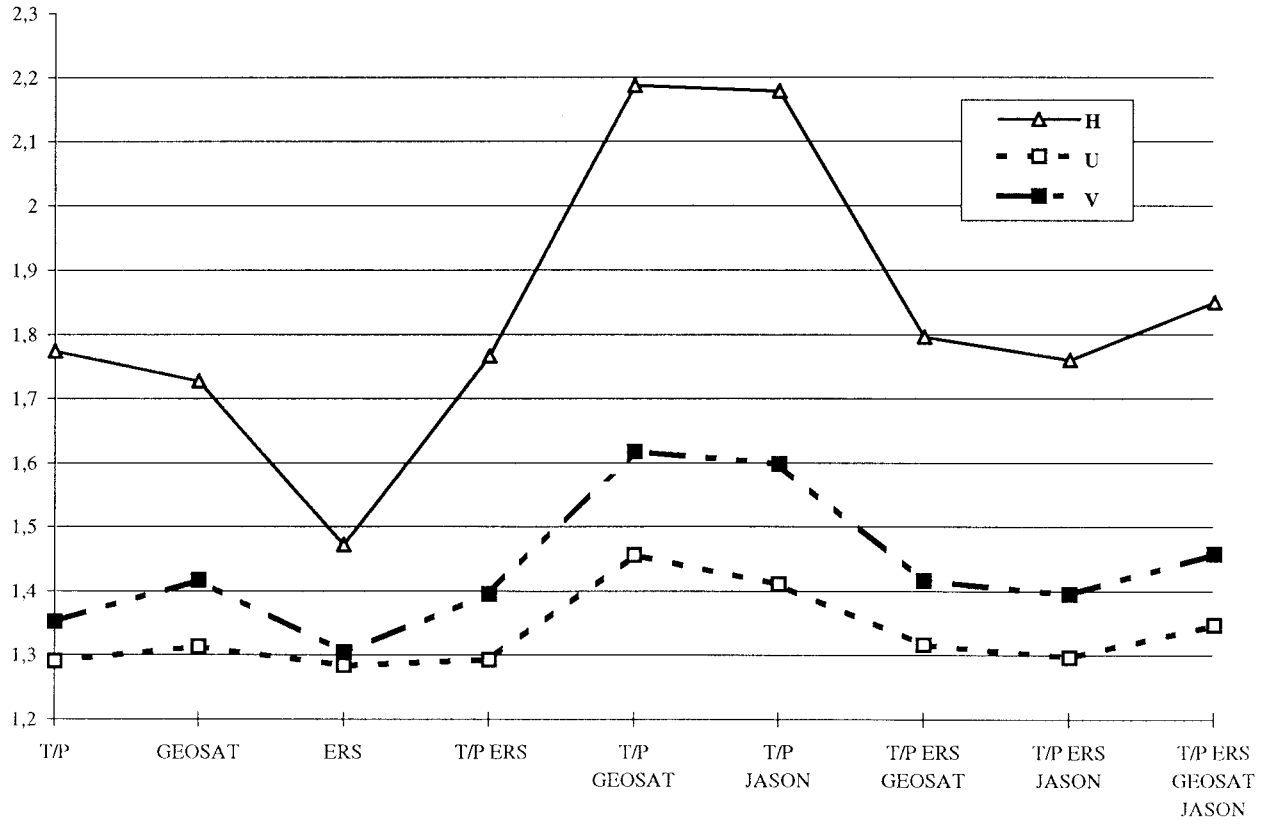

FIG. 9. Ratio of the *H* mean mapping error for the (10°–20°) latitude band over the *H* mean mapping error for the nominal (40°–50°) latitude band.

inal case (L = 150 km, T = 15 days). They are thus only approximations of the actual (i.e., here derived from model fields) covariance functions. Such a choice is more representative of a real mapping exercise. Note that the signal mapping (contrary to the formal error estimation) is not very sensitive to this a priori choice because the constraint from the data is strong. The noise level was set to 1% (i.e., corresponding to near-perfect data).

Comparison of the reconstructed fields with the reference model fields allows an estimation of the mapping error. The main interest of such a simulation is that it allows us to visualize the mapping errors, while our formal errors only give a statistical estimation. This can help to determine whether mapping errors are acceptable or not. Figure 10 shows the POCM sea level anomaly (relative to a 3-yr mean) for a particular day in the year and the same field but reconstructed from T/P, ERS, T/P + ERS, T/P + *Jason-1*, and T/P + ERS + GFO simulated along-track data. The POCM signal ranges from −24 to +16 cm and corresponds to meanders, rings, or eddies of the Gulf Stream extension. The signal is qualitatively well recovered with all configurations. Only the T/P case shows clear difference with the reference field. The differences with the reference field are shown on Fig. 11. The rms difference is 1.49, 0.66, 0.52, 0.51, and 0.49 cm for T/P, ERS, T/P + ERS, T/P + *Jason-1*, and T/P + ERS + GFO, respectively. The signal variance is about 50 cm^2, which means that the relative mapping errors (in percentage of signal variance) are all below 1%, except for T/P. For a statistically more representative estimation, the mapping errors were calculated over one year both for the sea level *H* and the *U* and *V* geostrophic velocities. Results are summarized in Tables 1 and 2. They confirm the results derived from the previous example. With two satellites or more, the error on the sea level is less than 1 cm rms or less than 1% of the signal variance. POCM mesoscale fields are thus extremely well resolved in the Gulf Stream extension with multiple-altimeter missions. More interestingly, the velocity fields are also very well reconstructed with a mapping error of about 1 cm s^{-1} for a signal variance of about 100 $cm^2\ s^{-2}$ (i.e., a relative error of about 1% of the signal variance).

The mapping capability varies in space and time. Some configurations have a mapping error very stable in time (e.g., T/P, T/P + *Jason-1*), while others have complex space/time variations of mapping errors (GFO, ERS). To complement the previous illustrations, we show the evolution in time of mapping error at a given location for the different satellite configurations. The point location is situated between two T/P crossovers.

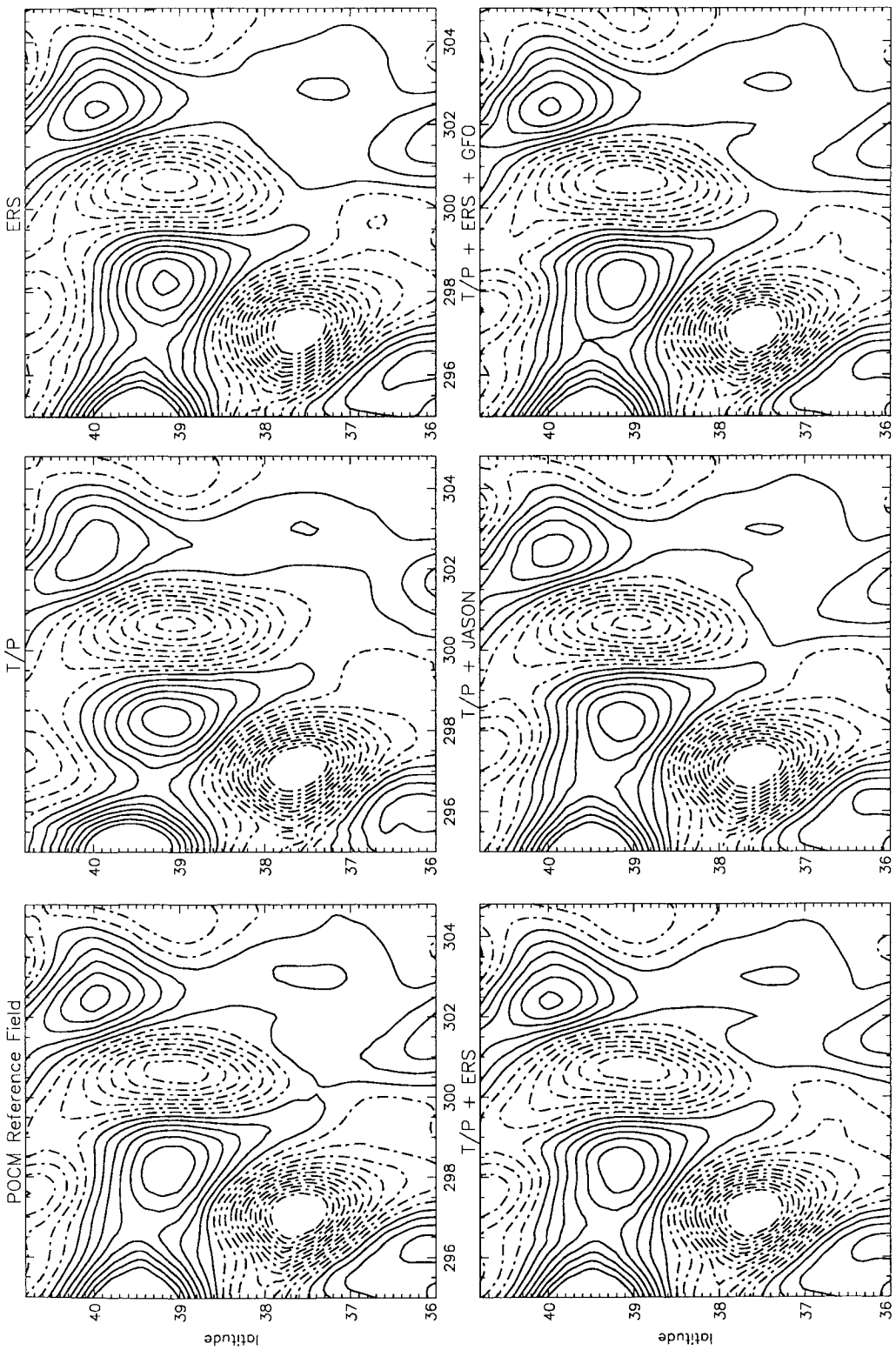

FIG. 10. Comparison of POCM sea level anomaly field (reference field) with maps reconstructed from T/P, ERS, T/P + ERS, T/P + *Jason-1*, and T/P + ERS + GFO along-track sampling. Contour interval is 2 cm.

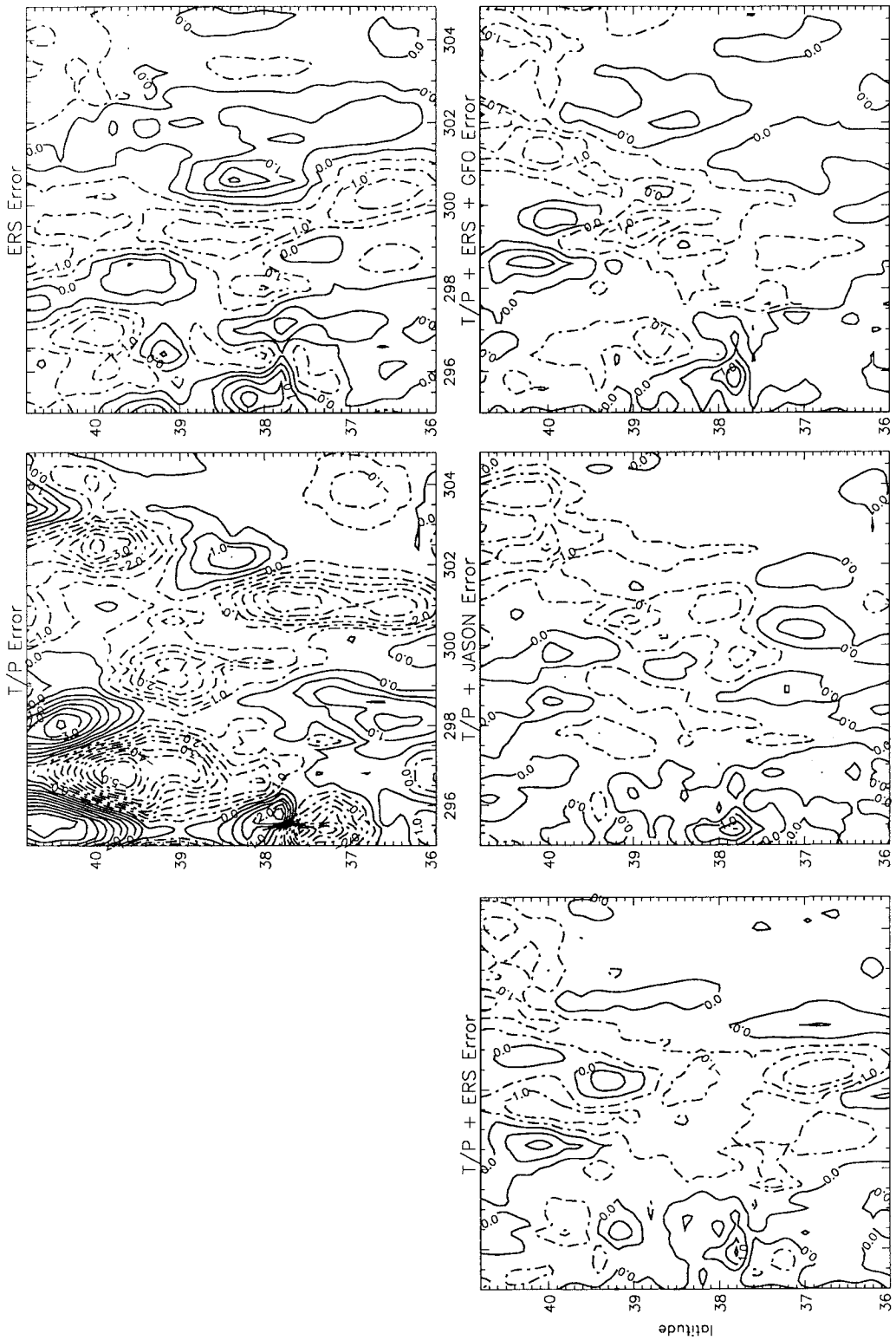

FIG. 11. Differences between the reconstructed maps and the reference field for T/P, ERS, T/P + ERS, T/P + *Jason*-1, and T/P + ERS + GFO. Contour interval is 0.5 cm.

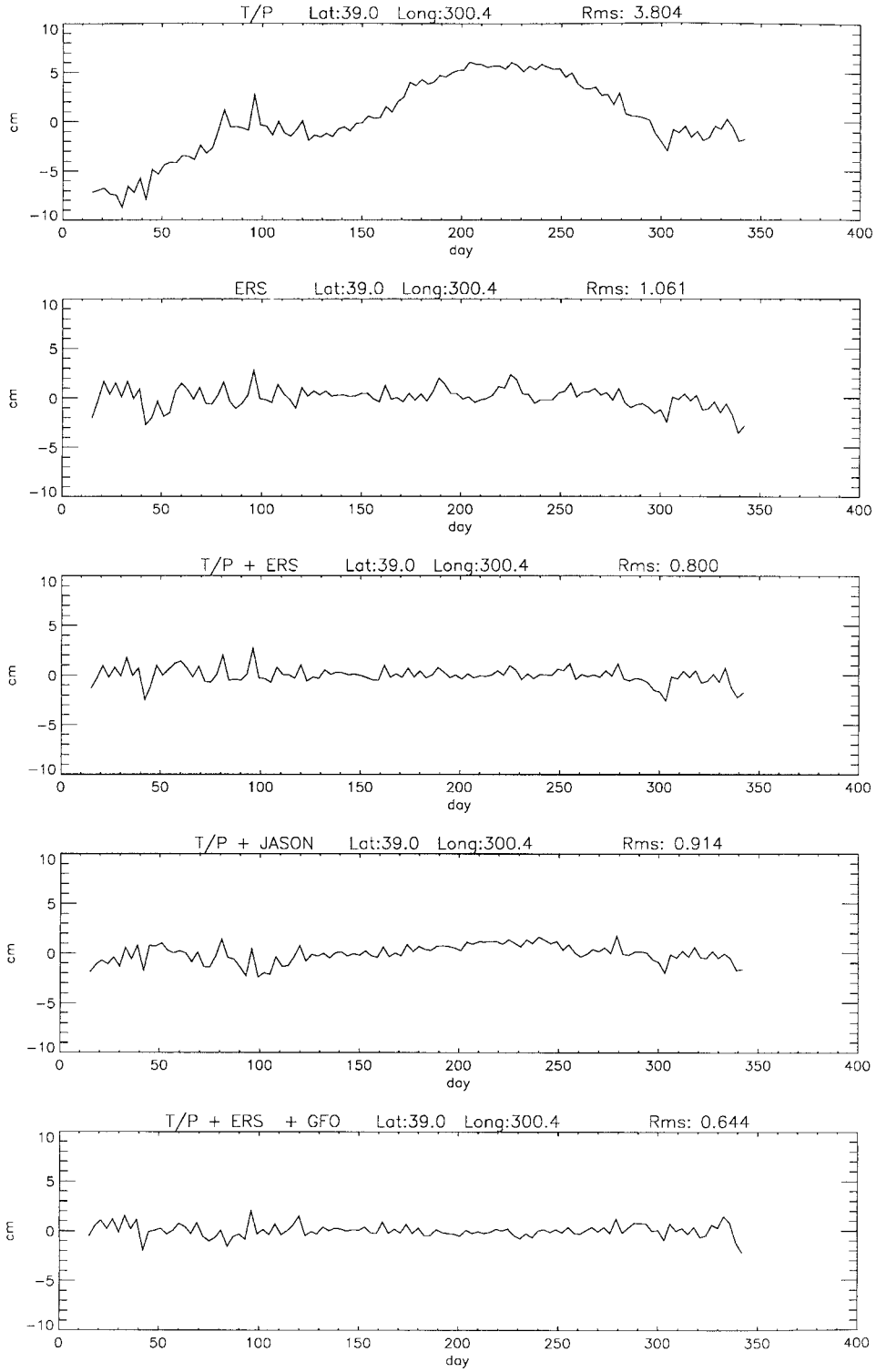

FIG. 12. Evolution of the mapping error at a given location (39°N, 300.4°E) for T/P, ERS, T/P + ERS, T/P + *Jason-1*, and T/P + ERS + GFO. Units in cm.

TABLE 1. Root-mean-square mapping error for *H*, *U*, and *V* (difference between POCM sea level anomaly and maps reconstructed from along-track simulated altimeter data) over one year. Units are in cm for *H* and in cm s^{-1} for *U* and *V*.

	H (cm)	*U* (cm s^{-1})	*V* (cm s^{-1})
TP	1.9	2.7	3.5
ERS	0.9	1.2	2.2
TP + ERS	0.7	1.0	1.4
TP + *Jason-1*	0.6	0.9	1.1
TP + ERS + GFO	0.6	0.8	1.2

TABLE 2. Same as Table 1 but differences are given in percentage of the signal variance.

	H (%)	*U* (%)	*V* (%)
TP	8.4	13.9	12.8
ERS	1.5	2.1	3.7
TP + ERS	0.8	1.2	1.6
TP + *Jason-1*	0.7	1.1	1.1
TP + ERS + GFO	0.6	0.9	1.1

The T/P error is, of course, large (3.8 cm rms), ERS error is smaller (1 cm rms), T/P + *Jason-1* and T/P + ERS have similar errors (0.8 and 0.9 cm rms, respectively), and the combination of T/P + ERS + GFO has the smallest error (0.64 cm rms). The two- and three-satellite combinations thus have rms errors below 1 cm with maximum errors generally below 2 cm. Such mapping errors are much lower than the signal, which has an rms of 8.5 cm and maximum/minimum values between −18 and +15 cm. Thus, the variations in time of the mapping errors will not be a problem for interpreting the reconstructed ocean signal. These variations are actually more representative of very short timescale events in the model fields rather than time inhomogeneity of the mapping error. Results are different at other locations and, in particular, the ranking of the different configurations will change (e.g., at a T/P crossover point, T/P will obviously perform better than the combination of *Jason-1*, ERS, and GFO). They all show, however, that the mapping errors are always sufficiently low compared to the ocean signal when at least two satellites are combined.

These simulations thus confirm the conclusions derived from our formal error analyses. They show that the mesoscale signals are well resolved with at least two satellites. Mapping errors derived from these simulations are even much smaller than the ones derived from our formal error estimates. This can be explained by the large space and timescales of POCM sea level anomaly fields. The very good results on the velocity estimations are also probably due to the absence of small-scale signals in POCM data. It is clear, however, that the mesoscale variability is not well simulated by POCM (e.g., Stammer et al. 1996). Our previous formal error estimates are thus probably a more reliable estimation of the actual mesoscale variability mapping errors.

5. Conclusions

The mesoscale mapping capability of sea level anomaly, and zonal and meridional velocity by existing or future altimeter missions was analyzed. A large number of simulations was performed, including studies of sensitivity to correlation function, a priori noise, and latitude. The main conclusions are as follows.

- The Geosat (or GFO) orbit provides the best sea level and velocity mapping for the single-satellite case for all the simulations we performed.
- In most simulations the *Jason-1* + T/P (interleaved T/P–*Jason-1* tandem orbit scenario) provides the best mapping for the two-satellite case. There are few differences, however, with respect to the T/P + ERS or T/P + Geosat scenario. The T/P + Geosat configuration actually performs better for a few simulations, particularly for the velocity field mapping. The gain provided by an optimized two-satellite (*Jason-1* + T/P) configuration relative to a nonoptimized configuration (T/P + ERS or T/P + Geosat) is thus not very large. Also, the T/P + ERS or T/P + Geosat configurations have the advantages of providing data at higher latitudes.
- The conclusions differ from those of Greenslade et al. (1997), mainly because of their definition of resolution (standard deviation of error had to be very small compared to mean error). As a result, only the large-scale signal can be ''resolved.'' Greenslade et al. (1997) thus show that the T/P + *Jason-1* combination performs much better than a nonoptimized two-satellite combination (such as T/P + ERS) for large-scale signal mapping. Greenslade et al. (1997) also conclude that the mesoscale signal cannot be mapped with an acceptable accuracy from present and future multiple-altimeter missions. A resolution definition is a fundamentally subjective choice, however, and our analyses show that the mesoscale signal can be rather well or well mapped from multiple-altimeter missions. Although the mapping errors are not homogeneous, they remain sufficiently small relative to the signal. They are also a priori known, which should avoid any misinterpretation of results.
- There is a large improvement in sea level mapping when going from one satellite to two satellites. Compared to T/P, the combination of T/P and ERS has, for example, a mean mapping error reduced by a factor of 4 and a standard deviation reduced by a factor of 5. Compared to ERS or even Geosat, the reduction is smaller but still a factor of more than 2. The improvement in sea level mapping is not as large when going from two to three or three to four satellites. Compared to the Geosat, ERS, and T/P mean mapping errors, the *Jason-1* + T/P mean mapping error is, respectively, reduced by 5%, 9%, and 17% of the signal variance. The reduction in mean mapping error by going from two to three and from three to four sat-

ellites is, however, only 1.5% and 0.7% of the signal variance, respectively. This also holds if a much smaller a priori noise is assumed (2% instead of 10%).

- The velocity field mapping is more demanding, however, in terms of sampling. The *U* and *V* mean mapping errors are two to four times larger than the *H* mapping error. Their error structure is also very different from the *H* error structure. The contribution from a third satellite is also more significant than for *H*. Only a combination of three satellites can actually provide a velocity field mapping error below 10% of the signal variance. Mapping of the meridional velocity is less accurate but by only 10% to 20% even at low latitudes. This suggests that the criterion of a satellite orbit with a rather low inclination for a better estimation of the velocity field is not really relevant, particularly for a multisatellite configuration.
- These results are confirmed using POCM model data. POCM *H*, *U*, and *V* fields in the Gulf Stream extension are very well reconstructed from along-track altimeter data when at least two satellites are used. This is partly due, however, to the large space and timescales of POCM mesoscale variability.

The study also shows that the *Jason*-1–T/P orbit tandem scenario should be optimized by taking the other satellites (GFO and ENVISAT) into account. It also confirms what is generally agreed as being the main requirement for future altimeter missions, that is, that at least two (and preferably three) missions are needed with one very precise long-term altimeter system (such as T/P and later on *Jason*-1) to provide a reference for the other missions.

Acknowledgments. This study was partly supported by a CNES contract. We wish to thank Philippe Escudier and Nicolas Ducet for useful discussions on this work. M. Schlax kindly provided us with his own archive of POCM data, which he got from R. Tokmakian.

APPENDIX

Comparison of Mapping Error on *H* and *U* or *V*

To better understand the relationship between the mapping error on *H* and *U* or *V*, it is instructive to analyze the simple example of a north–south track. In this case, ε_u^2, the variance on the error on *u*, is simply given by

$$\varepsilon_u^2 = 2(g/f)^2\varepsilon_H^2/L_1^2, \quad \text{(A1)}$$

where ε_H^2 is the *H* error variance (assumed to be uncorrelated) and L_1 is a scale over which the derivative should be calculated. It has to be much smaller than the scale of the correlation function.

On the other hand, we can show (e.g., Le Traon and Hernandez 1992) that, given our choice of $C(r, t)$, the $H(\sigma_H^2)$ and $U(\sigma_u^2)$ variances are related as follows:

$$\sigma_u^2 = (2/3)(g/f)^2\sigma_H^2/(L/3.34)^2. \quad \text{(A2)}$$

Equations (A1) and (A2) yield

$$\varepsilon_u^2/\sigma_u^2 = 3\varepsilon_H^2/\sigma_H^2[(L/3.34)L_1]^2. \quad \text{(A3)}$$

Here, $(L/3.34)L_1$ should be around unity, which means the relative mapping error on *U* (or *V*) should be typically three times greater than the mapping error on *H*. This is only a crude estimation of the expected ratio. In reality, the situation will be different because of the track inclination, the presence of neighboring tracks, and mainly because ε_H cannot be assumed to be uncorrelated.

REFERENCES

Blayo, E., T. Mailly, B. Barnier, P. Brasseur, C. Le Provost, J. M. Molines, and J. Verron, 1997: Complementarity of *ERS-1* and TOPEX/Poseidon altimeter data in estimating the ocean circulation: Assimilation into a model of the North Atlantic. *J. Geophys. Res.*, **102,** 18 573–18 584.

Bretherton, F., R. Davis, and C. Fandry, 1976: A technique for objective analysis and design of oceanographic experiments applied to MODE-73. *Deep-Sea Res.*, **23,** 559–582.

Chassignet, E. P., W. R. Holland, and A. Capotondi, 1992: Impact of the altimeter orbit on the reproduction of oceanic rings: Application to a regional model of the Gulf Stream. *Oceanol. Acta*, **15,** 479–490.

Dukowicz, J. K., and R. D. Smith, 1994: Implicit free-surface method for the Bryan–Cox–Semtner ocean model. *J. Geophys. Res.*, **99,** 7991–8014.

Greenslade, D. J. M., D. B. Chelton, and M. G. Schlax, 1997: The midlatitude resolution capability of sea level fields constructed from single and multiple satellite altimeter datasets. *J. Atmos. Oceanic Technol.*, **14,** 849–870.

Hernandez, F., P. Y. Le Traon, and R. Morrow, 1995: Mapping mesoscale variability of the Azores current using TOPEX/Poseidon and *ERS-1* altimetry, together with hydrographic and Lagrangian measurements. *J. Geophys. Res.*, **100,** 24 995–25 006.

Le Traon, P. Y., 1991: Time scales of mesoscale variability and their relationship with spatial scales in the North Atlantic. *J. Mar. Res.*, **49,** 1–26.

——, and F. Hernandez, 1992: Mapping of the oceanic mesoscale circulation: Validation of satellite altimetry using surface drifters. *J. Atmos. Oceanic Technol.*, **9,** 687–698.

——, and F. Ogor, 1998: *ERS-1/2* orbit improvement using TOPEX/Poseidon: The 2-cm challenge. *J. Geophys. Res.*, **103,** 8045–8057.

——, F. Nadal, and N. Ducet, 1998: An improved mapping method of multisatellite altimeter data. *J. Atmos. Oceanic Technol.*, **15,** 522–534.

Morrow, R., R. Coleman, J. Church, and D. B. Chelton, 1994: Surface eddy momentum flux and velocity variances in the Southern Ocean from Geosat altimetry. *J. Phys. Oceanogr.*, **24,** 2050–2071.

Stammer, D., 1997: Global characteristics of ocean variability estimated from regional TOPEX/Poseidon altimeter measurements. *J. Phys. Oceanogr.*, **27,** 1743–1769.

——, R. Tokmakian, A. Semtner, and C. Wunsch, 1996: How well does a 1/4° global circulation model simulate large-scale oceanic observations? *J. Geophys. Res.*, **101,** 25 779–25 812.

Wunsch, C., 1989: Sampling characteristics of satellite orbits. *J. Atmos. Oceanic Technol.*, **6,** 892–907.